Materials Science Forum Vols. 510-511 (2006) pp. 654-657
online at http://www.scientific.net

A Study of Ga_2O_3 Nanomaterials Synthesized by the Thermal Evaporation of GaN Powders

Hyoun Woo Kim[a], Ju Hyun Myung and Seung Hyun Shim

School of Materials Science and Engineering

College of Engineering, Inha University

253 Yong Hyun Dong, Nam Gu, Incheon 402-751, Republic of Korea

[a]email: hwkim@inha.ac.kr

Keywords: Thermal Evaporation, Gallium Oxide, Nanomaterials.

Abstract. We have synthesized gallium oxide (Ga_2O_3) nanomaterials at two different growth temperatures on iridium (Ir)-coated substrates by thermal evaporation of GaN powders. The products consist mainly of nanobelts, with some additional nanosheets. The nanobelts were of a single-crystalline monoclinic Ga_2O_3 structure. The broad emission photoluminescence band of 900°C-products had a different peak position from that of the 970°C-products.

Introduction

After the discovery of carbon nanotubes, nanostructured materials have drawn much attention for their novel physical properties and technological significance for nanoelectronics and optoelectronics [1-6]. Since Ga_2O_3 is a widegap compound with intense luminescence properties [3] and since the belt-like nanostructure may be an ideal system for fully understanding dimensionally confined transport phenomena and fabricating functional nanodevices, some researchers have prepared Ga_2O_3 nanobelts by thermally heating or evaporating Ga_2O_3 powders mixed with active carbon/carbon nanotubes [7] or with graphite [8], GaN powders [9,10], a mixture of Ga and Ga_2O_3 powders [11], etc. To the best of our knowledge, there are few reports on the effect of temperature on the properties of Ga_2O_3 nanomaterials.

In this paper, we describe the production of β-Ga_2O_3 belt-like structures on Ir layers at two different temperatures and investigate the effect of the growth temperature on the structural and optical properties. Thermal evaporation of GaN powders was used.

Experiments

The 99.99%-pure GaN powders and the substratewere placed on the lower and the upper holder , respectively, in the vertical tube furnace. We used thermally grown SiO_2 on Si(001) as a starting material onto which a layer of Ir (about 150 nm) was deposited. The powder-to-substrate distance was 5 mm. The furnace was heated and then maintained at temperatures in the range of 900-970°C for 2 h under a constant flow of nitrogen (N_2), before being cooled to room temperature.

The crystal structure of the products was analyzed using x-ray diffraction (XRD) (X'pert MRD-Philips) with $CuK\alpha_1$ radiation (λ = 0.154056 nm). The morphology and structure of the products were characterized using scanning electron microscopy (SEM) (Hitachi S-4200) and transmission electron microscopy (TEM) (Philips CM-200). TEM specimens were prepared by sonicating in acetone, and subsequently dropping onto a holey carbon film supported on a copper grid. Photoluminescence (PL) measurement was performed at room temperature using a He-Cd (325 nm, 55 mW) laser as the excitation light source.

Results and discussion

Fig. 1a and 1b are the cross-sectional SEM images showing the thin layers of wool-like material at growth temperatures of 900°C and 970°C, respectively. They revealed that the average thicknesses are about 33.5 μm and 84 μm. The materials consist of an agglomeration of one-dimensional (1-D) nanostructures with random growth directions. Fig. 1c shows the plan-view SEM image of the deposits at 900°C, consisting of nanobelts with various widths. Fig. 1d shows the plan-view SEM image of the deposits at 970°C, revealing that they are composed of wider nanobelts or nanosheets as well as nanobelts. Statistical analysis of many SEM images reveals that the deposits at 900°C and 970°C, respectively, have widths in the range of 100 nm-1 μm and 100 nm-7 μm.

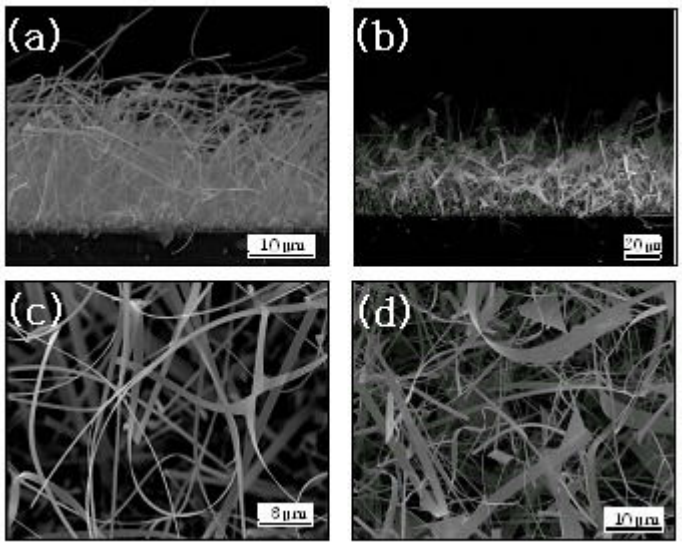

Fig. 1 (a,b) Cross-sectional and (c,d) Plan-view SEM images of the products, deposited at a growth temperature of (a,c) 900°C and (b,d) 970°C. nlarging the boxed region of the nanobelt shown in Fig. 2b. (d) Corresponding SAED pattern.

Fig. 2 shows a typical XRD pattern of the product at 970°C, on an Ir-coated substrate. The XRD pattern of the product at 900°C was similar to that at 970°C. The diffraction peaks in the pattern can be indexed to the monoclinic structured Ga_2O_3, which are in good agreement with the reported values of β-Ga_2O_3, with the lattice constants a=5.80Å, b=3.04Å, c=12.23Å, and β=103.7° (JCPDS Card No.11-370). Additionally, (111) diffraction peaks of Ir and the (0004) peak of Si (not shown here) from the substrate were detected. It is noteworthy that the (110) diffraction peak of GaIr was also found.

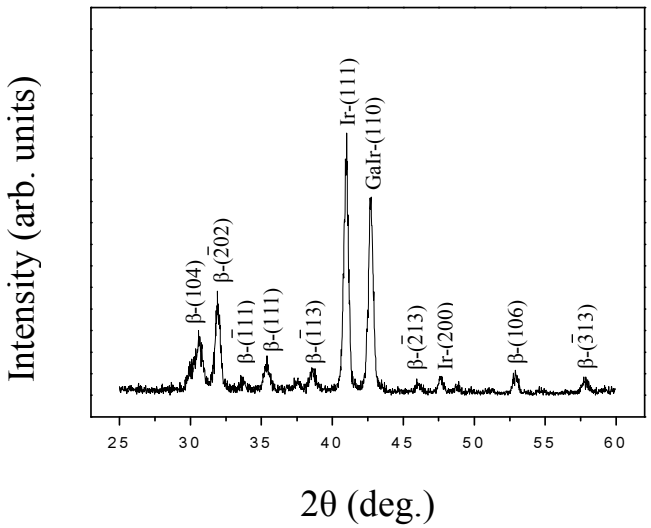

Fig. 2 XRD pattern recorded from the products on an Ir-coated substrate.

Fig. 3a shows the TEM image of a typical nanobelt and the corresponding selected area electron diffraction (SAED) pattern, recorded perpendicular to the nanobelt long axis. The nanobelts have almost uniform widths and smooth surfaces. The SAED pattern can be indexed for the $[01\bar{1}]$ zone axis of crystalline β-Ga_2O_3. The length direction of the nanobelt, indicated by an arrow, is along the [100] direction.

Fig. 3b is a high resolution TEM (HRTEM) image of the nanobelt shown in Fig. 3a, indicating that the Ga_2O_3 nanobelt is single crystalline. The interplanar spacing is about 0.56 nm, corresponding to the (100) planes of monoclinic β-Ga_2O_3.

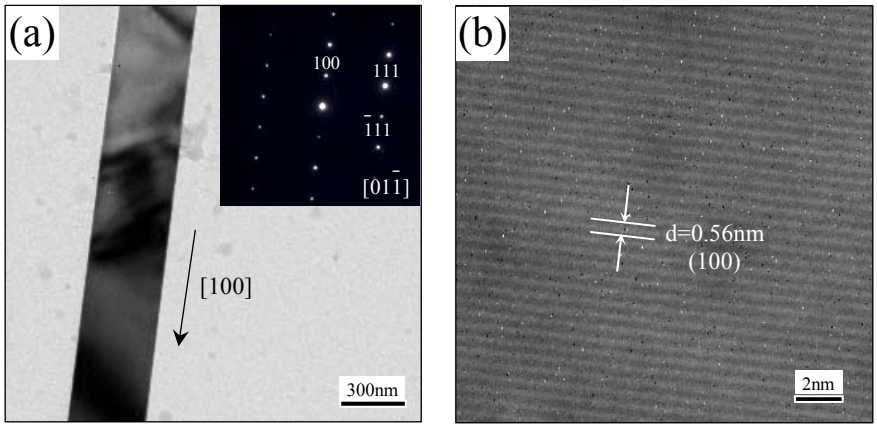

Fig. 3 (a) TEM image of a single β-Ga_2O_3 nanobelt. The inset shows the corresponding SAED pattern recorded along the [$01\bar{1}$] zone axis. (b) HRTEM image.

Since the GaIr diffraction peak as well as the Ir diffraction peaks was observed, it is likely that some of the Ga generated from the GaN powder reacts with Ir to form the GaIr compound. However, we could not observe any metal nanoparticles on the nanobelt tips and stems by SEM and TEM (not shown here) and thus we suppose that both Ir and GaIr remain on the substrate surface during the synthesis process. Therefore, the growth of nanomaterials in the present work is not controlled by the tip-growth vapor-liquid-solid mechanism, but by the vapor-solid mechanism [13]. The Ga atoms from GaN powders may react with O atoms, resulting in the formation of Ga_2O_3 nanobelts. The oxygen in the Ga_2O_3 has been probably come from the air leakage or the residual oxygen in the furnace. It is known that the degree of supersaturation in the gaseous phase influences the morphologies of the product [14]. At the higher temperature of 970°C, a larger amount of Ga vapor may be evaporated from the Ga source and subsequently transported to the substrate, providing the condition of higher supersaturation and the material nucleate more evenly, resulting in the occurrence of wider nanobelts or nanosheets. Intensive investigation is required to derive the more detailed mechanism for the formation of Ga_2O_3 nanomaterials in the present work.

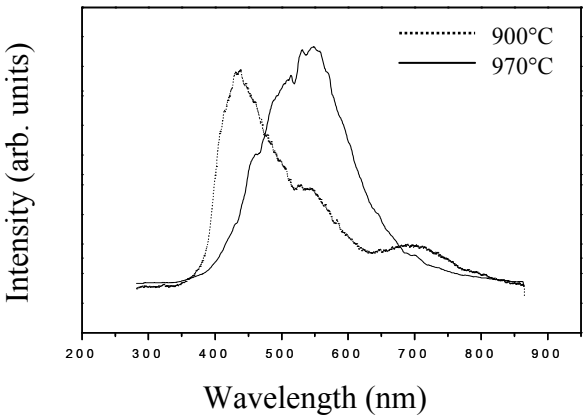

Fig. 4 Room temperature PL spectra of the products at growth temperatures of 900°C and 970°C with an excitation wavelength of 325 nm.

Fig. 4 shows the room temperature PL spectra of the deposits at growth temperatures of 900 and 970°C. For both growth temperatures, there is an apparent broad emission PL band, which can be a superimposition of several peaks. The PL band centered at about 435 nm corresponds to the products at 900°C [15], while that centered at about 530 nm corresponds to the products at 970°C. We suppose that the blue shift of 900°C-deposits compared with 970°C-deposits is attributed to the dimensional decrease and quantum size effects [11,16]. The PL spectra of Ga_2O_3 are known to originate from the recombination of an electron on a donor formed by oxygen vacancies and a hole on an acceptor formed by gallium vacancies or gallium-oxygen vacancy pair [17,18]. According to Binet and Gourier [19], after excitation of the acceptor, a hole on the acceptor and an electron on a donor recombine radiatively and emit a blue photon. Additionally, we observe the red peak centered at around 700 nm, arising from intrinsic impurities or nitrogen incorporation during the evaporation process under the N_2 gas flow [20].

Summary

In summary, we synthesized Ga_2O_3 nanomaterials, such as nanobelts and nanosheets through a thermal evaporation method of heating GaN powders under N_2 flow. SEM revealed that the morphology of the products is affected by the substrate temperature, and that wider nanomaterials can be synthesized at a higher temperature. TEM revealed that the obtained β-Ga_2O_3 nanobelts are single crystallines and grow along the [100] direction. In addition, the PL spectra showed that the peak position of the broad emission bands depends on the substrate temperature.

Acknowledgements

This work was supported by Korea Research Foundation Grant (KRF-2004-003-D00141).

References

[1] E. W. Wong, P. E. Sheehan and C. M. Lieber: Science Vol. 277 (1997), p.1971.

[2] J. T. Hu, T. W. Odom and C. M. Lieber: Acc Chem Res Vol. 32 (1999), p. 435.

[3] Z. W. Pan, Z. R. Dai and Z. L. Wang: Science Vol. 291 (2001), p. 1947.

[4] L. F. Dong, J. Jiao, D. W. Tuggle, J. Petty, S. A. Elliff and M. Coulter: Appl Phys Lett Vol. 82 (2003), p. 1096.

[5] L. Wang, X. Zhang and F. Zeng: Mater. Sci. Forum Vol. 475-479 (2005), p. 3535.

[6] Z. Xie, W. Yang, H. Miao, L. Zhang and L. An: Mater. Sci. Forum Vol. 475-479 (2005), p. 1239.

[7] G. Gundiah, A. Govindaraj and C. N. R. Rao: Chem Phys Lett Vol. 351 (2002), p. 189.

[8] J. Zhang and L. D. Zhang: Solid State Commun vol. 122 (2002):p. 493.

[9] J. S. Lee, K. Park, S. Nahm, S. W. Kim and S. Kim: J Cryst Growth Vol. 244 (2002), p. 287.

[10] Z. R. Dai, Z. W. Pan and Z. L. Wang: J Phys Chem B Vol. 106 (2002), p. 902.

[11] J. Zhang, F. Jiang and L. D. Zhang: Phys Lett A Vol. 322 (2004), p. 363.

[12] B. Y. Geng, L. D. Zhang, G. W. Meng, T. Xie, X. S. Peng and Y. Lin: J Cryst Growth Vol. 259 (2003), p. 291.

[13] X. Xiang, C. B. Cao, Y. J. Guo and H. S. Zhu: Chem Phys Lett Vol. 378 (2003), p. 660.

[14] J. Guojian, Z. Hanrui, Z. Jiong, R. Meiling, L. Wenlan, W. Fengying and Z. Baolin: J Mater Sci Vol. 35 (2000), p. 63.

[15] H. W. Kim and N. H. Kim: Appl Phys A, Vol. 80 (2005), p. 537.

[16] C. H. Liang, G. W. Meng, G. Z. Wang, Y. W. Wang, L. D. Zhang and S. Y. Zhang: Appl Phys Lett Vol. 89 (2001), p. 3202.

[17] T. Harwig and F. Kellendouk: J Solid State Chem Vol., 24 (1978), p. 255.

[18] V. I. Vasil'tsiv, Y. N. Zakharko and Y. I. Prim: Ukr Fiz Zh Vol. 33 (1988), p. 1320.

[19] L. Binet and D. Gourier: J Phys Chem Solids Vol. 59 (1998), p. 1241.

[20] Y. P. Song, H. Z. Zhang, C. Lin, Y. W. Zhu, G. H. Li, F. H. Yang and D. P. Yu: Phys Rev B Vol. 69 (2004), p. 075304.